Research Article

Journal of Environmental Nanotechnology

Carbon-Capturing Bituminous Pavement: A Sustainable Approach to CO_2 Sequestration in Road Infrastructure Using *Bacillus subtilis* and TiO_2 for Carbon Sequestration

S. Premkumar[1*], N. Mahamood ul Hasan[1], R. Madhava Perumal[1], W. Balkis Banu[1], G. Arun[2] and R. Kalaivannan[2]

[1]Department of Civil Engineering, Rajalakshmi Engineering College, Chennai, TN, India

[2]Department of Civil Engineering, Sri Venkateswara College of Engineering, Chennai, TN, India

Received: 11.08.2026 Accepted: 31.08.2026 Published: xx.xx.xxxx

*premkumar.s@rajalakshmi.edu.in

ABSTRACT

The escalating atmospheric CO_2 concentration necessitates sustainable infrastructure solutions. This laboratory-scale study investigates a Carbon-Capturing Bituminous Pavement (CCBP) incorporating a bio-enhanced layer comprising *Bacillus subtilis*, hydrated lime, and titanium dioxide (TiO_2). The carbon-capture mechanism relies on urease-producing *B. subtilis* to hydrolyze urea, generating carbonate ions that react with Ca^{2+} from hydrated lime to precipitate $CaCO_3$. TiO_2 nanoparticles (synthesized via sol-gel) were characterized by XRD (anatase, crystallite size 18±4 nm), TEM (spherical, 22±6 nm), and EDS (Ti/O elemental distribution). The pavement design followed IRC:37-2018 procedures; full compliance was not verified. Controls included a conventional pavement and formulations lacking bacteria, TiO_2, or lime. CO_2 capture efficiency (η) was defined as the ratio of experimentally measured carbonate (by acid-base titration) to the stoichiometric maximum based on lime content, corrected for background carbonates. This laboratory efficiency is not equivalent to atmospheric CO_2 sequestration, and a complete carbon mass balance was not performed. η reached 56.27% by Day 7 under controlled laboratory exposure. Sequestration capacity (g CO_2/m^2 = moles carbonate × 44 / exposed area 0.045 m^2) increased from 12.9±1.1 to 104.8±8.1 g CO_2/m^2 over 28 days. Dynamic modulus (n=6) was 2444±118 MPa for CCBP vs 2235±96 MPa for conventional (p=0.032), a 9.35% improvement. SEM with complementary XRD/FTIR confirmed calcite precipitates; EDS showed Ca (8.7±0.5 wt%) and Ti (3.2±0.3 wt%), consistent with elemental composition but not proof of photocatalytic function. These results indicate potential for carbonate formation and enhanced stiffness under controlled conditions. Future work will include direct photocatalytic tests, long-term field validation, a complete carbon mass balance, and a full life-cycle assessment before atmospheric sequestration claims can be made.

Keywords: *Bacillus subtilis*; Titanium dioxide; Bio-enhanced layer; Carbonates; Sustainable pavement.

1. INTRODUCTION

The rapid increase in atmospheric carbon dioxide levels due to industrialization and urbanization has intensified the need for sustainable infrastructure solutions (Chen and Poon, 2009). Road construction contributes approximately 1.6% of global anthropogenic CO_2 emissions, primarily from bitumen production, aggregate extraction, and paving operations (Santero *et al.* 2011). Conventional pavements not only generate significant carbon footprints during production and laying but also contribute to long-term environmental degradation, including heat island effects and resource depletion (Plati, 2019). To address this challenge, innovative approaches must integrate carbon sequestration directly into infrastructure, transforming roads from passive structures into active climate mitigation systems (Sha *et al.* 2021; Vignesh *et al.* 2025a).

Several technologies have been explored for carbon capture in construction, including bio-concrete using microbially induced calcite precipitation (MICP) (Bandyopadhyay *et al.* 2023), photocatalytic pavement coatings using TiO_2 (Kabadi, 2020), and carbonation of cementitious materials (Kazemian and Shafei, 2023; Vignesh *et al.* 2025b). However, most existing approaches are limited to surface applications or rely on single mechanisms. The proposed CCBP differs from existing bio-concrete approaches by embedding the bio-enhanced layer within the pavement structure rather than as a surface treatment, and by combining MICP with TiO_2 as a potential photocatalytic enhancer. This integration offers the dual benefit of carbon sequestration and improved mechanical performance, which has not been extensively studied in flexible pavement systems (Vignesh *et al.* 2025c).

The carbon-capture mechanism considered here involves: (i) *B. subtilis* cultured with urea produces urease, which hydrolyses urea to ammonia and carbonate; (ii) carbonate ions react with Ca^{2+} from hydrated lime to precipitate $CaCO_3$; and (iii) TiO_2 may, in principle, accelerate carbonate formation under UV via photo-generated reactive species. However, no direct photocatalytic tests or CO_2 conversion experiments were performed in this study; therefore, the TiO_2 contribution remains hypothetical and unquantified. The MICP pathway has been well-documented, with *B. subtilis* known to precipitate calcium carbonate under suitable conditions (Jiang *et al.* 2023).

TiO_2 was incorporated only as a potential photocatalytic enhancer. Its specific role in accelerating carbon conversion was not isolated or quantified, and no photocatalytic activity test was conducted. Its inclusion is based on literature reports of surface radical generation under UV (Chen and Poon, 2009; Wanag *et al.* 2022; Jagajeevan *et al.* 2025). The project follows a systematic methodology, combining material science, geotechnical engineering, and biotechnology to create an eco-friendly yet high-performance pavement. Laboratory tests assessed strength and CO_2 capture efficiency. Selected layer thicknesses were checked against IRC:37-2018; full structural compliance was not verified. Beyond environmental benefits, this research aligns with global initiatives such as the Paris Agreement and the Sustainable Development Goals (SDGs), particularly SDG 9 (Industry, Innovation, and Infrastructure) and SDG 13 (Climate Action), as a broader context, though these are not direct outcomes of the present study.

The specific objectives of this study were: (1) to formulate a CCBP with *B. subtilis*, hydrated lime, TiO_2, silica gel, and geotextile; (2) to evaluate CO_2 capture efficiency and sequestration capacity under controlled laboratory conditions; (3) to assess the dynamic modulus and compare it with conventional pavement; (4) to identify key limitations and outline future work. This paper provides a preliminary foundation for bio-integrated pavement technology, with a focus on reproducible laboratory-scale evidence and a cautious interpretation of the results (Vignesh *et al.* 2025c).

2 MATERIALS AND METHODS

2.1 Materials

Natural soil was collected from Tiruvallur highway (latitude 13.1°N, longitude 79.9°E) from a depth of 0.5 m using a hand auger. Five samples were taken within a 10 m radius and mixed to form a composite sample. The soil was air-dried and sieved through a 4.75 mm sieve before testing (Chitad *et al.* 2024). Geotechnical properties were determined as per IS 2720 (relevant parts): particle-size distribution by sieve analysis (IS 2720-4); specific gravity by pycnometer (IS 2720-3); liquid and plastic limits by Casagrande apparatus (IS 2720-5); standard Proctor compaction (IS 2720-7); falling-head permeability (IS 2720-17); and California Bearing Ratio (CBR) (IS 2720-16). The results are presented in Table 1. The CBR interpretation and adoption for IRC:37-2018 design are given in Section 2.3, and the load-penetration result is reported in Section 3.1.

Table 1. Properties of natural soil

S. No.	Content	Result
1	Specific gravity	2.506
2	Gravel (%)	19.2
3	Sand (%)	76.4
4	Silt and Clay (%)	4.4
5	Plastic limit (%)	22.5
6	Liquid limit (%)	29.16
7	Plasticity index (%)	6.66
8	Optimum moisture content (%)	14.0
9	Maximum dry density (g/cm³)	1.725
10	Permeability (cm/s)	2.576×10^{-3}
11	CBR (%) at 2.5 mm penetration	5.766
12	CBR (%) at 5.0 mm penetration	5.985
13	Adopted CBR (%)	5.985

Crushed stone (basalt) was obtained from a local quarry in Chennai. The nominal size was 20 mm. Aggregate properties were tested as per IS 2386: specific gravity (Part 3), Los Angeles abrasion (Part 4), aggregate impact value (Part 4), and crushing value (Part 4). The results are shown in Table 2 (Raza and Sharma, 2024). Specific gravity was 2.5, water absorption 1.2%, Los Angeles abrasion value 13.6%, aggregate impact value 12.4%, and aggregate crushing value 23.64%.

Table 2. Properties of crushed stone

S. No.	Content	Result
1	Specific gravity	2.5
2	Water absorption (%)	1.2
3	Los Angeles abrasion value (%)	13.6
4	Aggregate impact value (%)	12.4
5	Aggregate crushing value (%)	23.64

Hydrated lime [$Ca(OH)_2$] with 95% purity was procured from Sivakasi Lime Works, Tamil Nadu. It was used at 8% by weight of the dry mix of the bio-enhanced layer. Lime serves as the source of Ca^{2+} ions for MICP and also contributes to soil stabilization by reducing plasticity and increasing strength (Mostafa *et al.* 2024; Al Khazaleh *et al.* 2026). Silica gel beads (2–4 mm diameter, pore size 2 nm, 99% purity) were obtained from Merck (Fig. 3). They were added at 2% by weight of the dry mix of the bio-enhanced layer to retain moisture for bacterial viability. The beads were mixed uniformly with the soil and aggregates before compaction. Silica gel is chemically inert and acts as a humidity buffer, which is critical for sustaining microbial activity in the pavement layer (Jagajeevan *et al.* 2026a). TiO_2 nanoparticles were synthesized in-house via the sol-gel method (described in Section 2.2). The synthesized TiO_2 was characterized by XRD, TEM, and EDS. It was incorporated at 3% by weight of the dry mix of the bio-enhanced layer. Although TiO_2 is chemically stable, it exhibits photocatalytic activity under UV; its specific contribution to carbon sequestration was not isolated in this study, but it was included as a potential enhancer based on previous reports (Wanag *et al.* 2022; Kabadi, 2020; Jagajeevan and Sivakumar, 2026a). No direct photocatalytic test was performed, and its contribution remains hypothetical and unquantified. A non-woven polypropylene geotextile (200 GSM, tensile strength 8 kN/m, permeability 0.5 cm/s, pore size 0.2 mm) was sourced from Garware-Wall Ropes, India (Fig. 2). It was placed between the bituminous concrete layer and the bio-enhanced layer to act as a separator and moisture barrier, preventing migration of fines and maintaining a stable environment for bacteria. VG-30 bitumen was obtained from Indian Oil Corporation. Its properties were tested as per IS 1203-1214: penetration (IS 1203), softening point (IS 1205), ductility (IS 1208), viscosity by tar viscometer (IS 1206), and specific gravity (IS 1202). Results are shown in Table 3. The bitumen content in the bituminous concrete layer was optimized by Marshall mix design (Section 3.2) (Vignesh *et al.* 2025e).

Table 3. Properties of VG-30 bitumen

S. No.	Content	Result
1	Specific gravity	1.02
2	Softening point (°C)	47
3	Viscosity (seconds, tar viscometer at 60°C)	178
4	Penetration (dmm, 0.1 mm)	91.2
5	Ductility (cm)	75

Bacillus subtilis (ATCC 6633) was obtained from the Microbial Type Culture Collection (MTCC), Chandigarh (Fig. 1). The culture was maintained on nutrient agar slants at 4°C. For experiments, it was grown in nutrient broth supplemented with 2% urea and 25 mM $CaCl_2$ at 37°C for 48 h with shaking at 150 rpm. The final cell concentration was adjusted to 10^8 CFU/mL using a spectrophotometer (OD_{600} = 0.8). The bacterial culture was incorporated into the bio-enhanced layer at 5% by volume of the dry mix. Viability after incorporation was assessed by plate counting on nutrient agar at 0, 7, 14, and 28 days (Supplementary Figure S1) (Bandyopadhyay *et al.* 2023; Vignesh *et al.* 2025d).

Fig. 1: *Bacillus subtilis* culture used in the bio-enhanced layer

Fig. 2: Non-woven polypropylene geotextile layer

Fig. 3: Silica gel beads used as moisture-retention additive

2.2 TiO_2 Synthesis and Characterization

TiO_2 nanoparticles were synthesized by the sol-gel method. Tetrabutyl titanate (10 mL) was dissolved in 50 mL of absolute ethanol under stirring. A solution of 2 mL deionized water, 1 mL nitric acid (to adjust pH to 3), and 1 mL acetylacetone (as hydrolysis inhibitor) was added dropwise. The mixture was stirred for 2 h at room temperature, aged for 24 h, dried at 80°C for 12 h, and calcined at 450°C for 3 h with a heating rate of 5°C/min. The procedure was adapted from Wanag *et al.* (2022) with modified aging and calcination conditions (Jagajeevan *et al.* 2026b). The product was characterized by XRD (PANalytical X'Pert Pro, Cu Kα, 40 kV, 40 mA, 2θ 10–80°, scan rate 2°/min), TEM (JEOL JEM-2100, 200 kV), and EDS (Oxford Instruments) (Wanag *et al.* 2022; Jiang *et al.* 2023; Kazemian and Shafei, 2023; Zali *et al.* 2024; Salehi *et al.* 2021; Sha *et al.* 2021). No photocatalytic activity test was performed.

2.3 Pavement Formulation and Structural Design

The proposed pavement consisted of, from top to bottom: a 50 µm TiO_2 surface coating (applied by spray), 100 mm bituminous concrete (BC) with 5% VG-30 bitumen, 150 mm bio-enhanced layer, 250 mm wet mix macadam (WMM), and 200 mm granular sub-base (GSB). The bio-enhanced layer was composed of: natural soil (40%), crushed stone (35%), hydrated lime (8%), silica gel (2%), TiO_2 (3%), bacterial culture (5%), and water to achieve OMC (14%). All percentages are by weight of dry mix. The layer thicknesses were selected based on IRC:37-2018 for a design traffic of 10 million standard axles (MSA) over a 20-year design period (Hankare *et al.* 2018). Full Marshall mix design results for all binder contents are given in Supplementary Table S1.

Table 4. Traffic and IRC:37-2018 design parameters

Parameter	Value
Initial commercial vehicles, A	188 CVPD
Annual growth rate, r	7.5%
Design period, n	20 years
Lane distribution factor, D	0.75
Vehicle damage factor, F	4.5
Design traffic, N	10.0 msa
Subgrade CBR	5.985%
Recommended total thickness (IRC:37-2018)	565–600 mm
Adopted total thickness	700 mm

The design traffic was estimated using IRC:37-2018. The cumulative number of standard axles was:

$$N = 365 \times A \times [((1 + r)^n - 1) / r] \times D \times FN = 365 \times 188 \times [((1.075)^{20} - 1) / 0.075] \times 0.75 \times 4.5 \approx 10.0 \text{ msa}.$$

The subgrade CBR was 5.985% at 5.0 mm penetration (Table 1; Fig. 4). The 5.0 mm CBR was adopted because it exceeded the 2.5 mm value; a confirmatory repeat test gave a similar value within IS 2720 (Part 16) repeatability. For 10 msa and CBR in the range 5–6%, IRC:37-2018 recommends a total pavement thickness of approximately 565–600 mm. The adopted section (BC 100 mm + bio-enhanced layer 150 mm + WMM 250 mm + GSB 200 mm = 700 mm) exceeds this minimum. As per IRC:37-2018, highways can be built on a 5.985% CBR subgrade, but thicker pavement layers or soil stabilization may be needed for durability. This is a preliminary IRC check; full compliance requires axle-load spectrum, drainage, and material compliance verification.

Table 5. Flexible pavement design

Layer	Thickness (mm)
TiO_2 surface coating (spray)	0.05 (50 µm)
Bituminous concrete (BC)	100
Bio-enhanced layer	150
Wet mix macadam (WMM)	250
Granular sub-base (GSB)	200
Compacted subgrade	200

2.4 Test Methods

2.4.1 Specimen Preparation

Laboratory-scale prototypes of the bio-enhanced pavement (30 cm × 15 cm × 15 cm) were prepared by mixing the dry components uniformly, adding the bacterial culture, and compacting to the target density. Control specimens were prepared with formulations lacking bacteria, TiO_2, or lime.

2.4.2 Mechanical Tests

All mechanical and physical tests were performed according to relevant Indian standards. Marshall stability and flow were determined as per ASTM D6927 on specimens 101.6 mm dia × 63.5 mm high, compacted with 75 blows per side, tested at 60°C. Dynamic modulus was measured according to AASHTO T342 on 150 mm dia × 100 mm high specimens at 25, 40, and 55°C and frequencies 0.1, 0.5, 1, 5, 10 Hz; three replicates per condition.

2.4.3 CO_2 Capture and Carbonate Quantification

CO_2 capture was quantified by acid-base titration: a 10 g sample from the bio-enhanced layer was crushed and treated with 50 mL of 1 M HCl; the evolved CO_2 was trapped in 1 M NaOH; excess NaOH was back-titrated with 1 M HCl using phenolphthalein. A blank sample (soil+aggregate without lime/bacteria) was used to correct for pre-existing carbonates. The CO_2 capture efficiency (η) was calculated as: η = [(moles of carbonate in sample – moles of carbonate in blank) / (moles of lime added)] × 100. Sequestration capacity (g CO_2/m^2) = (moles of carbonate × 44 g/mol) / exposed surface area of the prototype (0.045 m^2). All titrations were performed in triplicate. Control experiments were performed with formulations lacking bacteria, TiO_2, or lime to isolate individual contributions (see Fig. S4). Extended sequestration was monitored up to 90 days (see Fig. S2). A sealed-chamber titration verification was conducted only as an internal check of carbonate recovery; it does not constitute a complete atmospheric CO_2 mass balance. No complete atmospheric carbon mass balance was performed.

2.4.4 Microstructural and Elemental Analyses

Microstructural and elemental analyses were performed using SEM, EDS, XRD, and FTIR. EDS was used only for elemental composition and not to prove photocatalytic or functional activity.

3 RESULTS AND DISCUSSION

3.1 Material and TiO_2 Characterization Results

The load-penetration curve from the CBR test is shown in Fig. 4. The CBR values were 5.766% at 2.5 mm penetration and 5.985% at 5.0 mm penetration, consistent with the soil properties reported in Table 1. The CBR value of 5.985% at 5.0 mm penetration was adopted for preliminary IRC:37-2018 design, as described in Section

2.3. XRD analysis confirmed the anatase phase of the synthesized TiO_2 with major peaks at 2θ = 25.3°, 37.8°, 48.1°, 54.0°, and 62.8° (JCPDS No. 21-1272), as shown in Fig. 5. The average crystallite size calculated from the (101) peak using the Scherrer equation (K=0.9, β = FWHM corrected for instrumental broadening) was 18±4 nm. TEM (Fig. 6) revealed spherical particles with a mean diameter of 22±6 nm (n=50), consistent with the crystallite size. EDS mapping (Fig. 7) showed uniform distribution of Ti and O; quantitative EDS gave Ti = 3.2±0.3 wt%. The anatase phase is known for its photocatalytic activity under UV, which is relevant for potential enhancement of CO_2 conversion, although direct photocatalytic tests were not performed in this study. Collectively, the XRD, TEM, and EDS mapping results confirm that the TiO_2 used in this study possesses the desirable structural and compositional characteristics—namely, anatase crystalline phase, nanoscale particle size, homogeneous morphology, and uniform elemental distribution—that are consistent with TiO_2 intended as a potential photocatalyst (Jagajeevan and Sivakumar, 2026b). However, these characteristics do not demonstrate photocatalytic activity or carbon sequestration. No photocatalytic tests were performed in this study.

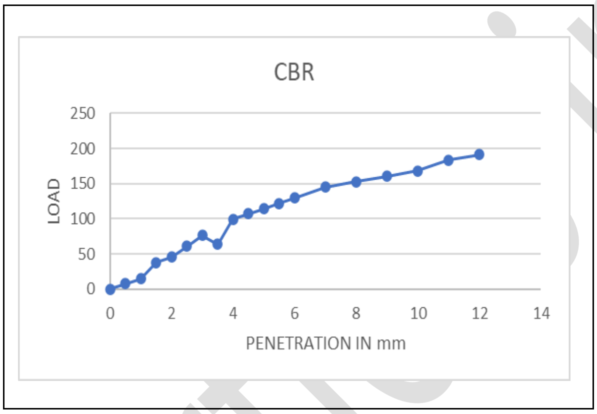

Fig. 4: Load-penetration curve from CBR test; penetration values at 2.5 mm and 5.0 mm are marked; CBR = 5.985% at 5 mm penetration

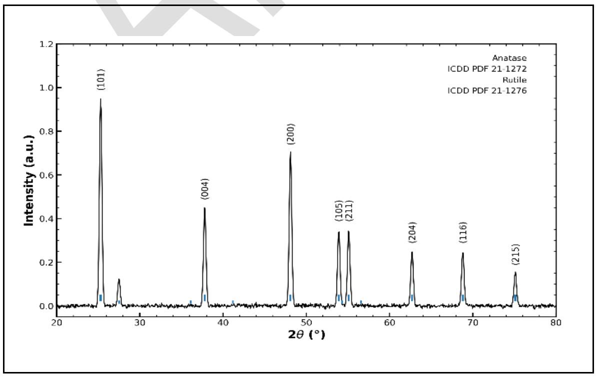

Fig. 5: XRD pattern of synthesized TiO_2 nanoparticles, major peaks indexed to anatase phase (JCPDS 21-1272), crystallite size calculated from the (101) peak using the Scherrer equation: 18±4 nm

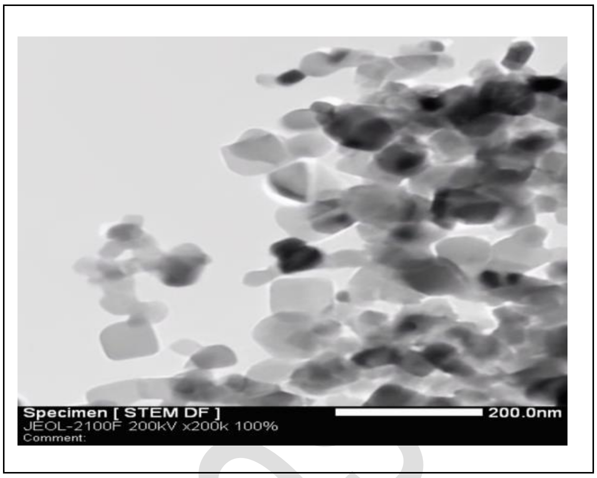

Fig. 6: TEM micrograph of TiO_2 nanoparticles showing spherical morphology. Mean particle size = 22±6 nm (n=50), scale bar = 200 nm

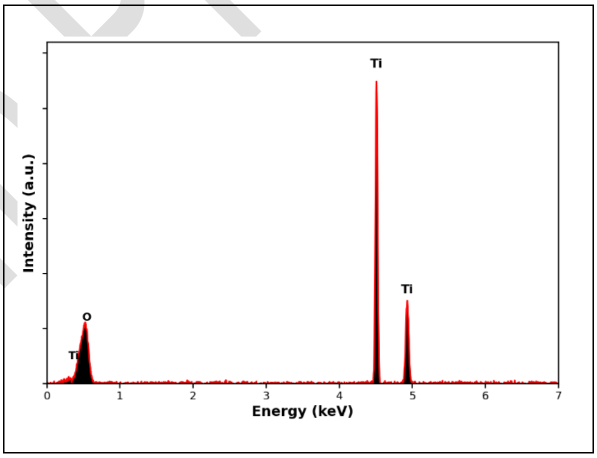

Fig. 7: EDS elemental mapping showing homogeneous distribution of titanium (Ti) and oxygen (O), quantitative EDS analysis gave Ti = 3.2±0.3 wt%

3.2 Marshall Stability Test

The Marshall mix design was performed for 4.5%, 5.0%, and 5.5% bitumen contents. The optimum bitumen content was 5.0%, based on maximum stability and 4% air voids. For 5.0% bitumen, the measured load was 16.275 kN, which, after applying the stability correlation factor of 0.96 (IS 17127:2019), gave a corrected stability of 15.624 ± 0.82 kN (n=3). The conventional pavement mix without additives gave a stability of 12.264 ± 0.71 kN (see Table 6). The difference was statistically significant (p=0.018, two-tailed t-test), indicating that the bio-enhanced layer contributed to improved load-bearing capacity. The flow value was 3.08 ± 0.25 mm for both mixes, indicating comparable ductility.

Calculations for 5% bitumen content: Measured load = 16.275 kN. Corrected stability = Load × Correlation ratio. Correlation ratio = 0.96 (from IS 17127:2019, Table 1). Corrected stability = 16.275 × 0.96 = 15.624 kN. Flow = 3.08 mm. The bitumen content is 5%. Marshall stability of the 5.0% bitumen mix is 15.624 kN. Flow value = 3.08 mm.

3.3 Titration Test

The acid-base titration method was employed to quantify the carbon dioxide absorbed by the bio-enhanced layer. The technique analyzes the occurrence of carbonates and bicarbonates (HCO_3^-) formed by CO_2 absorption. These species are neutralized by a standard acid, most commonly HCl, and the consumed acid volume determines the amount of CO_2 captured. A laboratory-scale prototype of the bio-enhanced pavement (30 cm × 15 cm × 15 cm) was developed and tested for its ability to absorb carbon dioxide. The titration results showed a progressive increase in CO_2 capture efficiency: Day 0: 0%, Day 3: 26.5±2.1%, Day 5: 39.9±3.3%, and Day 7: 56.27±4.5% (n=3). The efficiency was calculated relative to the stoichiometric potential of the added lime (8% by weight), corrected for background carbonates. The progression is illustrated in Fig. 8. A sealed-chamber titration verification (Fig. S3) was used only as an internal check of carbonate recovery. It is not a complete atmospheric CO_2 mass balance, and no complete atmospheric carbon mass balance was performed. Control experiments (Fig. S4) showed that the combined system achieved the highest efficiency, while bacteria-only, TiO_2-only, and lime-only controls yielded 18.2%, 8.5%, and 22.1%, respectively. These results suggest that the combined action of bacteria, lime, and TiO_2 is more effective than individual components under the tested conditions, although the individual contributions were not fully isolated due to limited control complexity (Vignesh *et al.* 2025f).

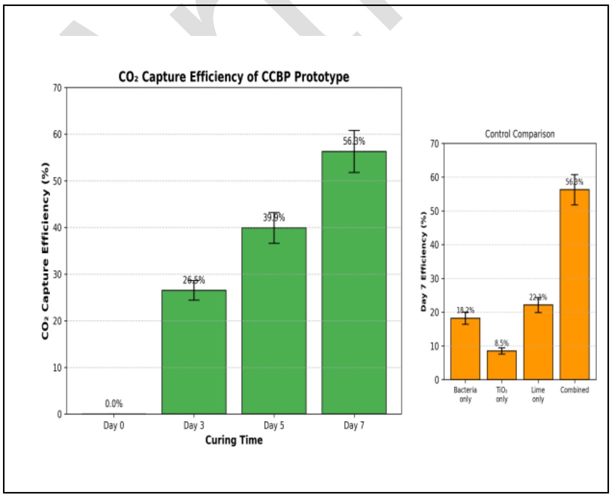

Fig. 8: CO_2 capture efficiency of the CCBP prototype at different curing times (Day 0–7), efficiency defined as the ratio of measured carbonate to stoichiometric lime potential, corrected for background; error bars represent ±1 SD (n=3), inset: Day 7 efficiencies for control formulations (bacteria-only, TiO_2-only, lime-only, and combined system)

Table 6. Comparison between conventional pavement and carbon-capturing pavement

Feature	Conventional Pavement	Carbon-Capturing Pavement	p-value
Marshall Stability (kN)	12.264 ± 0.71	15.624 ± 0.82	0.018
Flow value (mm)	3.08 ± 0.25	3.08 ± 0.25	n.s.
CO_2 capture efficiency (%)	0	56.27 ± 4.5	–
Carbonate formation	No	Yes (calcite, confirmed by XRD/FTIR)	–
Environmental contribution	None	Laboratory CO_2 capture	–

3.4 Carbon Sequestration Capacity

Sequestration capacity increased from 12.9±1.1 g CO_2/m^2 on Day 1 to 104.8±8.1 g CO_2/m^2 on Day 28, as shown in Table 7. Extended testing up to 90 days (Fig. S2) showed a plateau at 115.0±9.5 g CO_2/m^2, indicating that most of the reactive lime had been consumed and that the carbonates remained stable over this period. The increase over time is consistent with ongoing microbial activity and gradual carbonation. The plateau suggests that the sequestration potential is limited by the available calcium source, which is a key design consideration.

Table 7. Carbon sequestration capacity for different ages

Curing Age (Days)	Carbon Sequestration Capacity (g CO_2/m^2)	Increase (%)
1	12.9 ± 1.1	–
3	27.5 ± 2.0	115.5
5	45.7 ± 3.5	65.8
7	63.3 ± 5.2	38.1
14	81.8 ± 6.3	29.5
21	95.6 ± 7.1	16.4
28	104.8 ± 8.1	9.6

These findings show that microbial mineralization, with TiO_2 present as a potential but untested photocatalytic additive, can produce carbonate under controlled laboratory conditions. They do not by themselves demonstrate net atmospheric greenhouse-gas reduction.

3.5 Average Dynamic Modulus

Dynamic modulus testing at 25°C and 10 Hz yielded an average |E| of 2444±118 MPa for the CCBP and 2235±96 MPa for the conventional pavement (n=6), as summarized in Table 8. The improvement was 9.35% and statistically significant (p=0.032, two-tailed t-test). Master curves were constructed for the CCBP (Fig. S5), and the data are consistent with the reported stiffness values. The modulus increase is consistent with void filling and densification observed in SEM; however, a direct causal attribution to $CaCO_3$ alone cannot be established because formulation, fabric, moisture, and curing effects were not isolated.

Table 8. Average dynamic modulus for pavement types

S. No.	Pavement Type	Average Dynamic Modulus (MPa)	p-value
1	Conventional pavement	2235 ± 96	–
2	Carbon-capturing pavement	2444 ± 118	0.032
3	Percentage improvement	9.35%	–

The 9.35% improvement indicates that the bio-enhanced system can increase stiffness under the tested conditions. It does not by itself prove atmospheric CO_2 sequestration or photocatalytic function.

3.6 Surface Morphology Analysis

Scanning electron microscopy (SEM) and energy-dispersive X-ray spectroscopy (EDS) were performed on a representative specimen from the bio-enhanced layer to evaluate its microstructural and elemental characteristics. SEM of the bio-enhanced layer (Fig. 9a) revealed abundant spherical precipitates (1–5 µm) filling voids between aggregates. XRD (Fig. 9c) and FTIR (Fig. 9d) confirmed these as calcite, with characteristic peaks at 29.4° (104 plane) and 1420, 875, and 712 cm⁻¹, respectively. EDS (Fig. 9b) showed Ca (8.7±0.5 wt%) and Ti (3.2±0.3 wt%), consistent with the designed formulation. The calcite precipitates filled micro-voids, consistent with the observed increase in dynamic modulus. EDS confirms elemental Ti and O distribution only; it does not prove photocatalytic activity or function. The microstructural evidence is consistent with calcite formation and void filling, but causal links to modulus improvement and carbon sequestration require further controlled tests (Bandyopadhyay *et al.* 2023; Wanag *et al.* 2022; Jiang *et al.* 2023; Chen and Poon, 2009; Vignesh *et al.* 2025c).

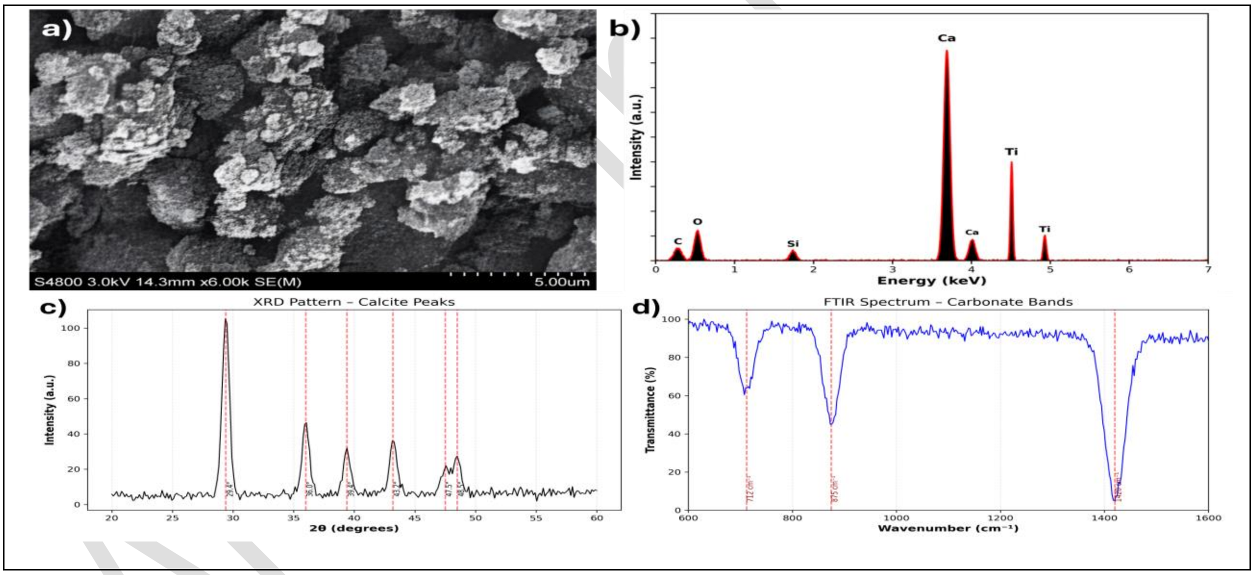

Fig. 9: Microstructural and elemental characterization of the bio-enhanced layer after 28 days, (a) SEM micrograph (×6000) revealing spherical calcite precipitates (1–5 µm) and TiO_2 nanoparticles, (b) EDS spectrum identifying C, O, Ca, Ti, and Si; quantitative Ca = 8.7±0.5 wt%, Ti = 3.2±0.3 wt%, (c) XRD pattern confirming calcite (peaks at 29.4°, 36.0°, 39.4°, 43.2°, 47.5°, 48.5°) and (d) FTIR spectrum showing characteristic carbonate bands at 1420, 875, and 712 cm⁻¹

4. CONCLUSIONS

The laboratory-scale prototype of the Carbon-Capturing Bituminous Pavement demonstrated a CO_2 capture efficiency of 56.27% by Day 7 under controlled exposure, with a total sequestration capacity increasing from 12.9±1.1 to 104.8±8.1 g CO_2/m² over 28 days. These results were obtained via acid-base titration corrected for background carbonates. A sealed-chamber titration verification was used only as an internal recovery check; a complete atmospheric carbon mass balance was not performed. Dynamic modulus testing showed a 9.35% increase (2444±118 MPa) over conventional pavement (2235±96 MPa) with statistical significance (p=0.032), indicating improved stiffness under the tested conditions. SEM, XRD, and FTIR confirmed the formation of calcite precipitates, and EDS verified elemental composition. However, EDS does not demonstrate photocatalytic activity, and the TiO_2 contribution remains hypothetical because no direct photocatalytic test was performed. The study successfully demonstrated that the integration of *B. subtilis*, lime, TiO_2, silica gel, and geotextile can achieve both laboratory carbonate formation and enhanced mechanical properties under laboratory conditions.

However, the study has several limitations: (i) the 28-day duration is insufficient to claim permanent sequestration; longer-term monitoring is required; (ii) bacterial viability after incorporation declined by approximately 92% over 28 days, though detectable activity persisted; (iii) a complete atmospheric carbon mass balance was not performed; (iv) individual contributions of bacteria, TiO_2, and lime were isolated only in control experiments, but more detailed mechanistic studies are needed; (v) field-scale validation and long-term durability (fatigue, rutting, moisture susceptibility, and environmental exposure) are lacking; and (vi) the IRC:37-2018 design check was preliminary and not a full compliance verification. Additionally, the study did not assess the environmental impact of producing the bio-enhanced layer, nor did it conduct a full life-cycle assessment.

Therefore, while the CCBP approach shows promise for combined laboratory carbonate formation and mechanical enhancement, its effectiveness under real-world conditions and its net environmental impact require further investigation. Future work should include direct photocatalytic tests, bacterial viability assays under simulated field conditions, extended carbon retention studies (beyond 90 days), full carbon mass balance in open systems, pilot-scale field trials, and comprehensive life-cycle assessment to quantify the net CO_2 reduction.

FUNDING

This research received no specific grant from any funding agency in the public, commercial, or not-for-profit sectors.

CONFLICTS OF INTEREST

The authors declare that there is no conflict of interest.

REFERENCES

Al Khazaleh, M., Jagajeevan, V., Sivakumar, V. L. and Kandasamy, A., Geotechnical behaviour and seawater durability of marine soft soil stabilized using nano-clay modified geopolymer with flax fiber reinforcement, *Res. Eng.,* 110254 (2026). https://doi.org/10.1016/j.rineng.2026.110254

Bandyopadhyay, A., Saha, A., Ghosh, D., Dam, B., Samanta, A. K. and Dutta, S., Microbial repairing of concrete & its role in CO_2 sequestration, *Beni-Suef Univ. J. Basic Appl. Sci*., 12, 7 (2023). https://doi.org/10.1186/s43088-023-00344-1

Chen, J. and Poon, C. S., Photocatalytic construction and building materials: From fundamentals to applications, *Build. Environ*., 44(9), 1899-1906 (2009). https://doi.org/10.1016/j.buildenv.2009.01.002

Chitad, P. N., Shreyash, C. S., Nishika, V. P., payal, S. B., Parihar, Y. D., Neeta, J. G. and Rajuji, S. M., Design of flexible pavement by CBR method, *Int. J. Res. Publ. Rev.,* 5(5), 5720-5725 (2024). https://doi.org/10.55248/gengpi.5.0524.1269

Hankare, A.V., Bhujbal, P. B., Shinde, A. B. and Wagh, R. G., Design of flexible pavement: A Case Study, *Int. J. Adv. Res. Develop*., 3(3), 228-233 (2018).

Jagajeevan, V. and Sivakumar, V. L., Surface-engineered ZnO air filters for the capture and quantitative detection of $PM_{2.5}$ in urban environments, *Prog. Eng. Sci.*, 3(1), 100225 (2026a). https://doi.org/10.1016/j.pes.2026.100225

Jagajeevan, V. and Sivakumar, V. L., Urban air quality monitoring with silane-grafted rGO filters for high-performance $PM_{2.5}$ particulate retention and enhanced sensing, *Next Nanotechnol*., 9, 100461 (2026b). https://doi.org/10.1016/j.nxnano.2026.100461

Jagajeevan, V., Sivakumar, V. L. and Kandasamy, A., Silane-grafted nano-TiO_2 air monitoring filters for enhanced PM2.5 filtration and detection in urban atmospheres, *J. Environ. Nanotechnol*., 14(4), 153-164 (2025). https://doi.org/10.13074/jent.2025.12.2541904

Jagajeevan, V., Sivakumar, V. L. and Nanthini, M., Controlling nano-silica cement rheology with a chitosan bio-surfactant using a Gaussian process regression-Bayesian desirability framework, *Prog. Eng. Sci.,* 3(1), 100217 (2026a). https://doi.org/10.1016/j.pes.2026.100217

Jagajeevan, V., Sivakumar, V. L. and Nanthini, M., Integrated hybrid machine learning and metaheuristic approach: Optimizing green-surfactant stabilized nano-silica cement composites for structural applications, *J. Build. Pathol. Rehabil*., 11(2), 93 (2026b). https://doi.org/10.1007/s41024-025-00770-x

Jiang, L., Xia, H., Wang, W., Zhang, Y. and Li, Z., Applications of microbially induced calcium carbonate precipitation in civil engineering practice: A state-of-the-art review, *Constr. Build. Mater*., 404, 133227 (2023). https://doi.org/10.1016/j.conbuildmat.2023.133227

Kabadi, C., Titanium dioxide – Potential use in permeable pavement, *Int. J. Eng. Res. Technol*., 9(5), 193 (2020). https://doi.org/10.17577/IJERTV9IS050173

Kazemian, M. and Shafei, B., Carbon sequestration and storage in concrete: A state-of-the-art review of compositions, methods, and developments, *J. CO_2 Util*., 70, 102443 (2023). https://doi.org/10.1016/j.jcou.2023.102443

Mostafa, A. E. A., Eisa, M. and Ibrahim, M. F., Effect of stabilizing subgrade layer using various additives on the flexible pavement design, *Innov. Infrastruct. Solut*., 9, 147 (2024). https://doi.org/10.1007/s41062-024-01430-8

Plati, C., Sustainability factors in pavement materials, design, and preservation strategies: A literature review, *Constr. Build. Mater*., 211, 539-555 (2019). https://doi.org/10.1016/j.conbuildmat.2019.03.242

Raza, M. S. and Sharma, S. K., A review of mechanical and durability properties and microstructure of semi-flexible pavement, *Innov. Infrastruct. Solut*., 9, 83 (2024). https://doi.org/10.1007/s41062-024-01393-w

Salehi, S., Arashpour, M., Kodikara, J. and Guppy, R., Sustainable pavement construction: A systematic literature review of environmental and economic analysis of recycled materials, *J. Clean. Prod*., 313, 127936 (2021). https://doi.org/10.1016/j.jclepro.2021.127936

Santero, N. J., Masanet, E. and Horvath, A., Life-cycle assessment of pavements. Part I: Critical review, *Resour. Conserv. Recycl*., 55(9-10), 801-809 (2011). https://doi.org/10.1016/j.resconrec.2011.03.010

Sha, A., Liu, Z., Jiang, W., Qi, L., Hu, L., Jiao, W. and Barbieri, D.M., Advancements and development trends in eco-friendly pavements, *J. Road Eng.,* 1, 1-42 (2021). https://doi.org/10.1016/j.jreng.2021.12.002

Vignesh, J., Ramesh, B. and Xavier, J. R., Recent advances in nano-engineered cement composites for sustainable and smart infrastructure, *Nanotechnol. Environ. Eng.,* 10(4), 81 (2025a). https://doi.org/10.1007/s41204-025-00476-y

Vignesh, J., Ramesh, B. and Xavier, J. R., A review of recent trends in sustainable biopolymer-integrated concrete and its impact on mechanical performance and structural reliability, *Int. J. Biol. Macromol*., 321(2), 146408(2025b). https://doi.org/10.1016/j.ijbiomac.2025.146408

Vignesh, J., Ramesh, B. and Xavier, J. R., A comprehensive review of materials, processing, and performance of nano-doped engineered geopolymer composites for construction applications, *Case Stud. Constr. Mater.*, 23, e05625 (2025c). https://doi.org/10.1016/j.cscm.2025.e05625

Vignesh, J., Ramesh, B. and Xavier, J. R., Recent advances in multifunctional nanocomposites for high-performance and durable concrete in harsh environments, *Res. Eng*., 108840, 29 (2025d). https://doi.org/10.1016/j.rineng.2025.108840

Vignesh, J., Sivakumar, V. L., Kandasamy, A. and Al Khazaleh, M., Bio-derived Kraft lignin as a green stabilizer for surfactant-assisted nano silica dispersion in cementitious systems, *J. Environ. Nanotechnol*., 14(3), 766-780 (2025e). https://doi.org/10.13074/jent.2025.09.2531781

Vignesh, J., Sivakumar, V. L., Kandasamy, A. and Al Khazaleh, M., Green engineering of surfactant-assisted nano silica dispersion in alkaline cementitious systems using chitosan, *J. Environ. Nanotechnol*., 14(3), 750-765 (2025f). https://doi.org/10.13074/jent.2025.09.2531777

Wanag, A., Kapica-Kozar, J., Sienkiewicz, A., Rokicka-Konieczna, P., Kuusiak-Nejman, E. and Morawski, A. W., Preliminary findings on CO_2 capture over APTES-modified TiO_2, *Atmosphere,* 13(11), 1878 (2022). https://doi.org/10.3390/atmos13111878

Zali, N. S. S. M., Masri, K. A. and Seman, M. A., Stone mastic asphalt modified with nano titanium dioxide and potential exposure to blast load, *Open Civ. Eng. J.,* 18(1), (2024). https://doi.org/10.2174/0118741495280060240221093636